UNEC Journal of Engineering and Applied Sciences
Vol. 4, No.2, 2024, pp. 5-11
DOI: https://doi.org/10.61640/ujeas.2024.1201

SECTION:
CHEMISTRY &
MATERIALS SCIENCE

The effect of matcha-impregnated sodium montmorillonite on the corrosion mitigation of mild steel in saline medium

M. Edraki[1], M. Sheydaei[2]*, A. Salmasifar[1], D. Zaarei[1]

[1]Department of Chemical and Polymer Engineering, South Tehran Branch, Islamic Azad University, Tehran 19585-466, Iran
[2]Department of Chemical Engineering, Faculty of Engineering, University of Garmsar, Garmsar, Iran
email: *mi_sheydaei@sut.ac.ir*

Abstract

Corrosion is a harmful phenomenon for metals, which causes a decrease in strength. Today, the use of plants as a green corrosion inhibitor has received much attention. Herein, using a cation exchange process, matcha (M) was incorporated into the structure of sodium montmorillonite (Na^+-MMT), and the anti-corrosion properties of the new nanoparticle (M-MMT) were investigated on mild steel in the saline solution phase. The results of Fourier transform infrared spectroscopy (FTIR), X-ray diffraction (XRD), and scanning electron microscopy (SEM) confirmed the authenticity of the new nanoparticle. The results of electrochemical impedance spectroscopy (EIS) and Raman spectroscopy showed that M-MMT improved the corrosion resistance. According to the results, matcha can be classified as considered a green inhibitor.

***Keywords*:** anticorrosion, green chemistry, environmental pollution, EIS.
PACS numbers: 78.70.Dm, 42.62.Fi

Received:	*Revised:*	*Accepted:*	*Published:*
24 June 2024	*16 July 2024*	*24 July 2024*	*26 December 2024*

1. Introduction

Mild steel is used in many different fields, for example, the main raw material in the manufacture of metal tools used in refineries, petrochemical plants, and agriculture [1,2]. Low cost, good formability, and adjustable surface hardness can be seen as advantages of mild steel, but its low corrosion resistance is a limiting and problematic issue [3-6]. Various techniques are used to increase the life of mild steel in harsh environments, but among them, corrosion inhibitors are used more [7-10]. They have many advantages, including fast reaction, high efficiency, and simple operation, and when used in very low concentrations, they can amazingly protect metal from damage [11]. In recent years, many plant extracts have been investigated as corrosion inhibitors [12, 13]. They are a non-toxic, low-cost, high-performance and environmentally friendly compound [14-16]. Doping the corrosion inhibitor into the structure of a host is a controlled release method [17, 18]. In fact, the inhibitor can be doped inside a neutral host structure, and by changing the pH or applying an external stress, the inhibitor is released and significantly prevents corrosion [19]. Montmorillonite (MMT) can be considered as one of the most important carriers [20, 21]. In fact, MMT is a member of nanoclay minerals and has properties such as the ability to expand in its interlayer spaces, which leads to swelling in the chemical structure [22]. Herein, matcha powder was loaded in the interlayer space of Na^+-MMT. The M-MMT was characterized by FTIR, XRD, and SEM.

Also, the anti-corrosion properties of M-MMT on mild steel in the saline solution phase were evaluated by EIS. Also, Raman spectroscopy were performed for confirming the inhibition performance.

2. Experimental

2.1. Materials

The Na^+-MMT, matcha powder, sodium chloride (NaCl), and substrates (mild steel) were obtained from Rockwood Company (USA), Arifoğlu Company (Türkiye), Merck Company (Germany), and Iranian Mobarakeh Steel Company, respectively.

2.2. Preparation of M-MMT

We prepared M-MMT by cation exchange process in an aqueous solution according to the method reported in the previous study [11].

2.3. MS substrate preparation and electrochemical tests (for solution study)

First, to remove contaminants, the samples (mild steel) were polished using SiC grinding papers and placed in an ultrasonic bath (with acetone and ethanol solution), and finally dried in hot air. In order to perform the electrochemical tests, an area of 1×1 cm^2 was selected as the surface in contact with the corrosive environment. To prevent rusting, the back and edges of substrates were covered via a mixture of Beeswax melt and colophony resin with a ratio of 2.5 to 1. To prepare the extract in a neutral medium (pH = 7), 1 g of M-MMT was dispersed in 1 liter of NaCl solution (3.5 *wt.*%) under a magnetic stirrer (with a rotational speed of 600 rpm) for 24 h. Finally, the pretreated steel samples for the corrosion test were immersed in the extract. The NaCl solution (3.5 *wt.*%) without M-MMT was used as the reference (blank) solution.

2.4. The measurements and characterization

A SEM (SEM-MIRAIII model-TESCAN company) was used to study the microstructure and morphology of Na^+-MMT and M-MMT. XRD measurements were carried out using an Xpert Pro MPD diffractometer. FT-IR spectra of the samples were recorded on an Equinox 55 spectrometer. Raman spectra of the samples were obtained on a TakRaman N1-541. A Potentiostat-galvanostat instrument (CorrTest CS350) was used for EIS test. A frequency range of 10 mHz to 10 kHz was selected for the EIS test. Nyquist and Bode diagrams were used to evaluate the corrosion resistance. Using two different electrolyres (M-MMT in NaCl solution and only 3.5 *wt*.% NaCl solution), three electrodes including a working electrode, a saturated calomel electrode (SCE), and an auxiliary electrode (Pt), were used in the electrochemical cell and the measurements were performed in the open circuit potential (OCP) and in the perturbation amplitude of ±10 mV. The Z Simpwin software was used to fit the equivalent diagrams. In this test, an area of 1 cm^2 of the prepared steel coupon was exposed to a solution containing 3.5% pure NaCl without the presence of any inhibitor and with the presence of M-MMT. Then, the above tests were performed at different immersion times (1, 4, and 24 h).

3. Results and discussion

3.1. Evaluation of matcha and M-MMT

FTIR and Raman methods were used to characterize matcha (see figure 1). In FTIR spectroscopy (a), peaks at around 1037, 1233, and 2853-2923 cm^{-1} are related to the C-O-C vibrations, -C-OH bending, and C-H stretching vibration, respectively [11]. The peaks at 1147 and 1383-1453 cm^{-1} are related to the C=O vibrations [2, 11]. Also, peaks at around 1633 and 3452 cm^{-1} are related to the -OH stretching vibration [11, 23-25]. In Raman spectroscopy (b),

the peaks at around 70, 1372-1572, and 2823-2944 cm^{-1} are corresponding to the -CO-NH-CH_3 vibrations, ring compounds (theophylline, theobromine, caffeine, catechin, epigallocatechin, gallocatechin gallate, epigallocatechin gallate), and CH_2 asymmetric stretching (including 4-aminobutyric acid, L-theanine), respectively [11].

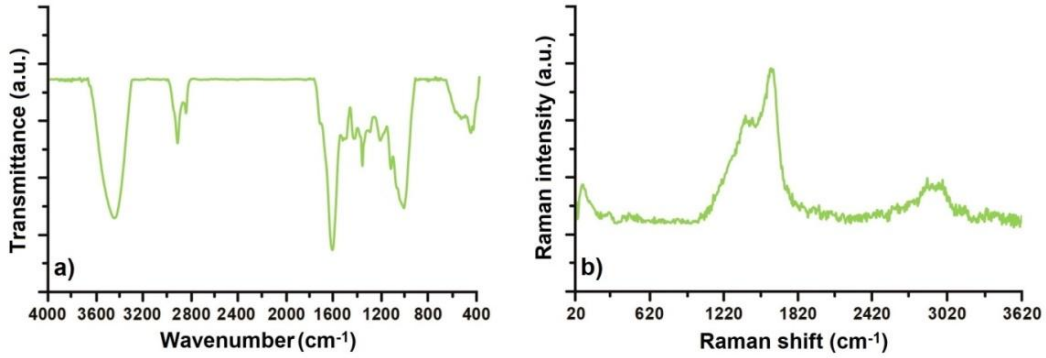

Figure 1. FTIR spectra (a) and Raman spectra (b) of matcha.

FTIR and XRD methods (see figure 2) were used to characterize of Na^+-MMT and M-MMT. The characteristic peaks (for FTIR) are reported in table 1. In the M-MMT spectrum, the rest of the peaks are related to the presence of MMT. XRD pattern (b) of Na^+-MMT consisted of one peak with a center at 2θ values around 6° (*d*-spacing = 10.92 Å) which is related to Na^+ cations [2,5,11]. But, the XRD pattern of the M-MMT consisted of one peak with a center at 2θ values around 5.1° (*d*-spacing = 16.14 Å). This change in XRD patterns is due to the absence of Na^+ cation and the presence of matcha in MMT.

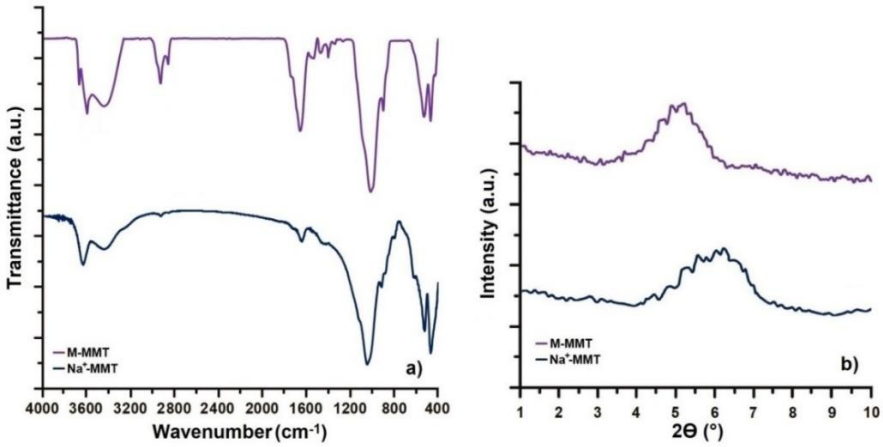

Figure 2. FTIR spectra (a) and XRD patterns (b) of Na^+-MMT and M-MMT.

Sample	Wavenumber (cm^{-1})	Characteristics	References
Na^+-MMT	465 and 1042	Bending and stretching Si-O vibrations	2
	522	Si-O-Al vibration and MgO groups	5
	914	Al_2OH bending groups	13
	1638-3446	Scissoring vibrations and symmetric vibrations of OH units	20,21
	3631	Stretching of OH (SiOH groups)	2,20,21
M-MMT	1228-1518	Ring compounds (theophylline, theobromine, caffeine, catechin, epigallocatechin, gallocatechin gallate, epigallocatechin gallate)	11
	2852	CH_2 asymmetric stretching (including 4-aminobutyric acid, L-theanine)	11

Table 1. Absorption peak characteristic of FTIR spectrum.

Figure 3 shows SEM images of samples. It can be seen that the morphology of M-MMT has changed to some extent. Almost the plates are partly separated, which this behavior reported in the literature [2].

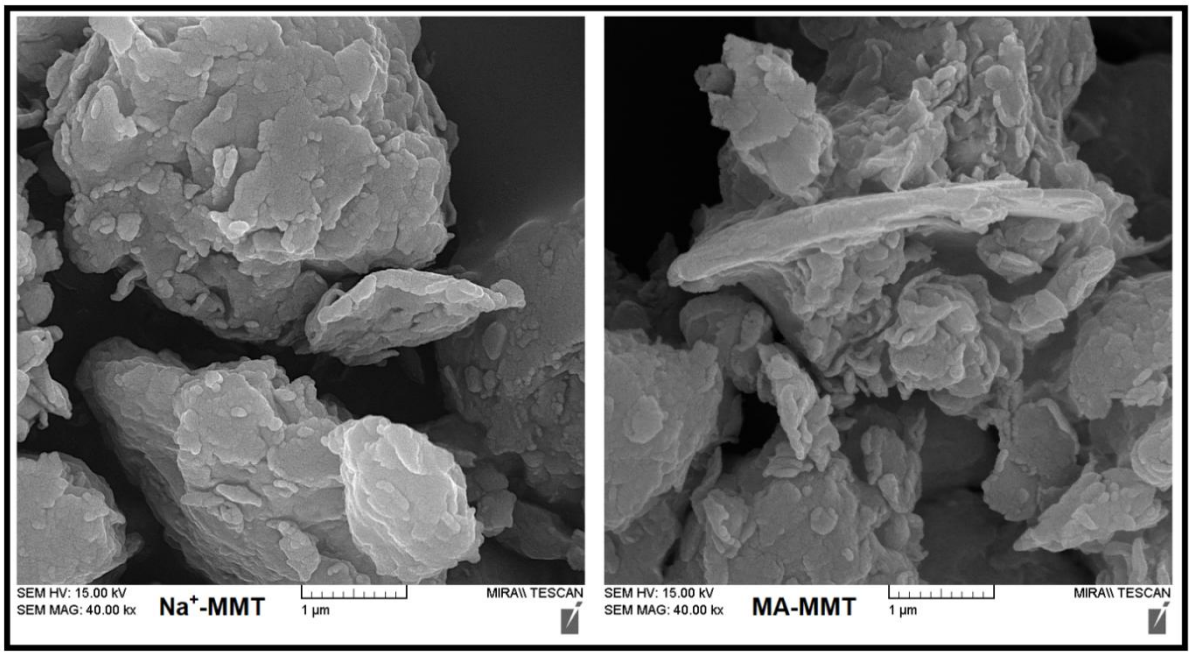

Figure 3. SEM images of samples.

3.2. Solution phase study

Figures 4 and 5, and table 2 show the results of the EIS test. The diameter of the curves (see figure 4) shows the charge transfer resistance (R_{ct}), the value of which for the blank sample decreased with time, which indicates its degradation in the NaCl solution. But, this value is increased for M-MMT which indicates corrosion resistance. Na^+-MMT, due to its hydrophilic nature, shows a rapidly decreasing R_{ct} value after immersion [2, 5, 11], so the increasing R_{ct} trend for M-MMT is due to the presence of matcha. In figure 5, the absolute value of the impedance at low frequencies is a measure of inhibition comparison [2, 20, 21], which decreases and increases over time for the blank and M-MMT samples, respectively. In fact, it is due to the interaction between the steel surface and the functional groups in M-MMT that the cathodic and anodic sites are occupied by these components and cause the surface to be passivated.

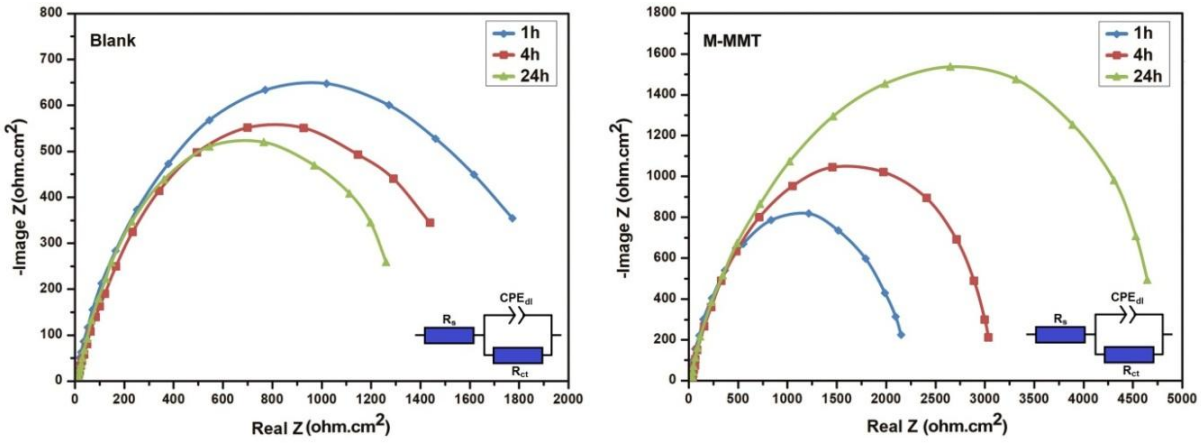

Figure 4. Nyquist plots for samples at different immersion times.

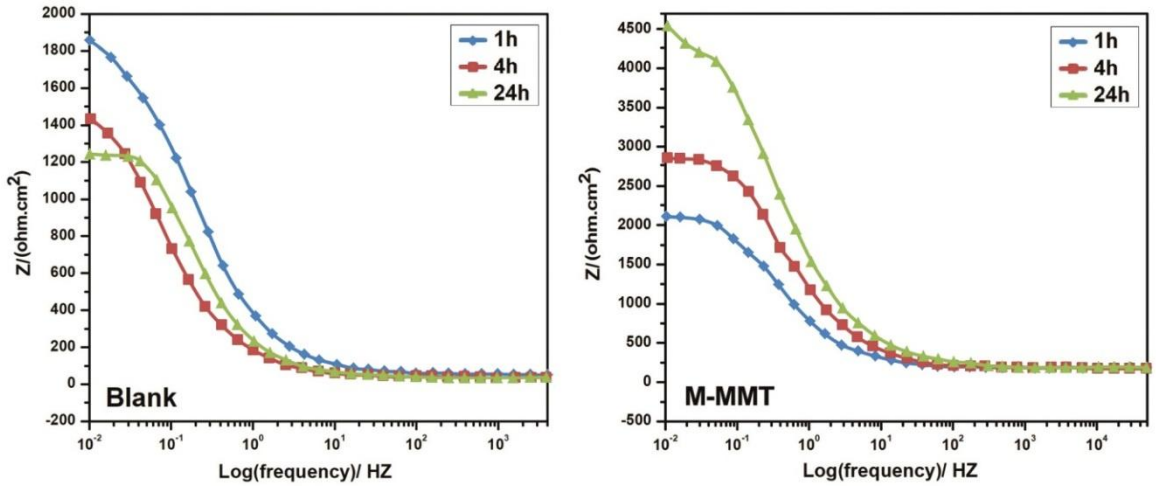

Figure 5. Bode plots for samples at different immersion times.

Solution	Time (h)	R_{ct}(a) (ohm.cm^2)	$Y_{0,dl}$ (b) (s^n. ohm^{-1}.cm^{-2})	n_{dl} (c)	R_s (ohm.cm^2)	C_{dl} (µF. cm^{-2})	log |z| ohm.cm^2	θ (%)	η (%)
Blank	1	1764.79	5.239×10^{-5}	0.77	7	39	1857.87	--	--
	4	1430.71	2.645×10^{-4}	0.77	7.8	47.6	1425.28	--	--
	24	1252.43	2.609×10^{-4}	0.78	7.5	94.2	1233.71	--	--
M-MMT	1	1916.17	1.398×10^{-4}	0.83	13	32.1	2018.23	17.69	8
	4	2713.32	5.276×10^{-5}	0.86	15	9.7	2798.73	79.62	48
	24	4161.68	1.613×10^{-5}	0.91	14	3	4558.55	96.81	70

Table 2. Electrochemical parameters extracted from the EIS results of steel samples immersed in the 3.5% NaCl solution with and without M-MMT.

In the circuits (see figure 4), R_s, R_{ct}, and CPE_{dl} represent the solution resistance, charge transfer resistance, and constant phase element in the electric double layer, respectively. Also, the capacitance of the electric double layer (C_{dl}) is obtained from equation 1 [26]. Moreover, $Y_{o,dl}$ and n represent the admittance of the constant phase element and the constant related to surface heterogeneity, respectively.

$$C_{dl} = Y_{0.dl}^{\frac{1}{n}} \left(\frac{R_s R_{ct}}{R_s + R_{ct}}\right)^{(1-n)/n} \quad (1)$$

Furthermore, the surface coverage (θ) and inhibition efficiency (η) were obtained using equations 2 and 3, respectively [27, 28].

$$\theta(\%) = 100\left(1 - \frac{C_{dl,M-MMT}}{C_{dl,Blank}}\right) \quad (2)$$

$$\eta(\%) = 100\left(1 - \frac{R_{ct,Blank}}{R_{ct,M-MMT}}\right) \quad (3)$$

According to the results reported in table 2, the minimum value of $Y_{o,dl}$ and C_{dl} for NaCl solution containing M-MMT was obtained after 24 h. In fact, this is due to the replacement of water molecules by matcha molecules, which are released from the interlayer distance of MMT during immersion at the metal/solution interface. Also, the reduction of C_{dl} is due to the absorption of matcha on the metal surface. The inhibition mechanism of matcha is due to the presence of functional groups such as carboxyl, amine, and thiol in the molecular structure of matcha. These groups have a pair of non-bonded electrons (such as the oxygen atom in

carboxyl, nitrogen atom in amine, and sulfur atom in thiol), which can exchange electrons with the surface, and they are absorbed on the surface [11]. In fact, it can be said that they block the anodic site by forming an insulating film [2, 5, 11]. In addition, MMT has the ability to react with OH^- at the cathodic site, and by forming an insoluble complex, it limits the access of O_2 to the cathodic site [2, 5, 19]. Raman spectroscopy was used to evaluate the products formed on the MS surfaces immersed in the saline solution with and without (blank) the presence of M-MMT after 24 h (see figure 7). According to the results, the characteristic peaks of iron oxides caused by the corrosion process are clearly seen for the blank sample. The peak located at 154 cm^{-1} confirms the symmetric stretch of the interlayer chloride ions in iron oxide [29]. The peaks at 215 cm^{-1}, 274 cm^{-1}, 393 cm^{-1}, 682 cm^{-1}, and 714-716 cm^{-1}, confirm the presence of hematite (α-Fe_2O_3), goethite (β-FeOOH)], lepidocrocide (γ-FeOOH), magnetite (Fe_3O_4), and maghemite (γ-Fe_2O_3) groups, respectively while the peaks at 1362 cm^{-1} and 1613 cm^{-1} are assigned to ferrihydrite ($Fe_5HO_8 4H_2O$) [29, 30]. Although the blank sample was full of corrosion products, a protective hybrid layer consisting of matcha and MMT was observed on the steel sample immersed in the saline solution containing M-MMT. The peaks at 430 cm^{-1}, 844 cm^{-1}, and 915 cm^{-1} indicate OH, MgAlOH, and AlOH functional groups, respectively, and the peak at 1100 cm^{-1} was assigned to Si-O. These four peaks are ascribed to MMT [2, 5, 11]. On the other hand, the peaks at 1371 cm^{-1} and 1570 cm^{-1} are attributed to ring compounds (phenolic components of matcha) [31]. Finally, the peak at 2915 cm^{-1} is assigned to the CH_2 asymmetric stretching functional groups of matcha [11, 31, 32].

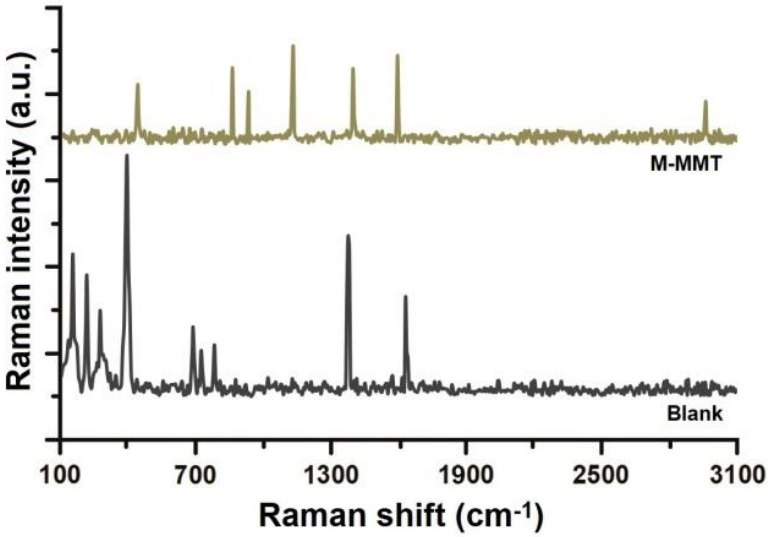

Figure 6. Raman spectra of the MS samples after 24 h immersion period in saline medium in the absence and presence of M-MMT.

4. Conclusion

To sum up, a corrosion inhibitor was prepared using matcha and Na^+-MMT. The results showed that M-MMT improves corrosion resistance. Environmentally friendly corrosion inhibitors are important because they are non-toxic and inexpensive. The results show that the use of plant compounds can be a suitable alternative to chemical inhibitors. Also, due to the non-toxicity of plant compounds, they can be used in many applications.

Authors'Declaration
The authors declare no conflict of interests regarding the publication of this article.

Funding
The authors did not receive support from any organization for the submitted work.

References

1. S.A. Haddadi, E. Alibakhshi, G. Bahlakeh, B. Ramezanzadeh, M. Mahdavian, Journal of Molecular Liquid **284** (2019) 682.
2. M. Sheydaei, M. Edraki, S.M. Radeghi Mehrjou, Gels **9** (2023) 490.
3. R.K. Suleiman, A.M. Kumar, A.Y. Adesina, F.A. Al-Badour, M.H. Meliani, T.A. Saleh, Corrosion Science **169** (2020) 108637.
4. D. Han, J. Li, N. Wang, K. Wan, International Journal of Electrochemical Science **15**(10) (2020) 9631.
5. M. Sheydaei, M. Edraki, S. Javanbakht, Polym Sci Ser B. **65** (2023) 991.
6. J.R. Beryl, J.R. Xavier, J. Bio- Tribo-Corros. **6** (2020) 126.
7. A.K. Hussain, N. Seetharamaiah, M. Pichumani, C.S. Chakra, Progress in Organic Coatings **153** (2021) 106040.
8. M. Edraki, M. Sheydaei, D. Zaarei, Chemical Review and Letters **6**(1) (2023) 79.
9. N. Arrousse, R. Salim, F. Benhiba, E.H. Mabrouk, A. Abdelaoui, F. El Hajjaji, I. Warad, A. Zarrouk, M. Taleb, Journal of Molecular Liquids **338** (2021) 116610.
10. M. Edraki, D. Zaarei, I. Sabeeh Hasan, Chemical Review and Letters **6** (2023) 428.
11. M. Sheydaei, M. Edraki, F.S.J. Abad, Iranian Polymer Journal **32**(12) (2023) 1643.
12. N. Hossain, M.A. Chowdhury, M. Kchaou, Journal of Adhesion Science and Technology **35**(7) (2021) 673.
13. M. Edraki, M. Sheydaei, E. Vessally, A. Salmasifar, Iranian Journal of Chemistry and Chemical Engineering **42**(9) (2023) 2775.
14. P. Ghahremani, M.E.H.N. Tehrani, M. Ramezanzadeh, B. Ramezanzadeh, Colloids and Surfaces A: Physicochemical and Engineering Aspects **629** (2021)127488.
15. M. Mahdavian, M.M. Attar, Prog. Color. Color. Coat. **8** (2015) 177.
16. G. Fekkar, F. Yousfi, H. Elmsellem, M. Aiboudi, M. Ramdani, I. Abdel-Rahman, B. Hammouti, L. Bouyazza, International Journal of Corrosion and Scale Inhibition **9**(2) (2020) 446.
17. M.H. Shahini, N. Taheri, H.E. Mohammadloo, B. Ramezanzadeh, Journal of the Taiwan Institute of Chemical Engineering **126** (2021) 252.
18. O. Razaghi Kashani, S. Amiri, M. Hosseini-zori, J. Nanostruct. **12**(3) (2022) 726.
19. M. Sheydaei, Surfaces **7**(2) (2024) 380.
20. M. Edraki, M. Sheydaei, Russian Journal of Applied Chemistry **95**(9) (2022) 1481.
21. M. Edraki, M. Sheydaei, D. Zaarei, A. Salmasifar, B. Azizi, Polymer Science, Series B. **64** (2022) 756.
22. M. H. Haghighat, A. Mohammad-Khah, Acta Chim. Slov. **67**(4) (2020) 1072.
23. M. Sheydaei, J. Sulfur Chem. **43**(6) (2022) 643.
24. M. Sheydaei, M. Edraki, E. Alinia-Ahandani, E. Nezhadghaffar-Borhani E, J. Sulfur Chem. **42**(6) (2021) 614.
25. M. Sheydaei, Polym. Sci. Ser. B. **65** (2023) 201.
26. M. Amini, R. Naderi, M. Mahdavian, A. Badiei, Microporous and Mesoporous Materials **315** (2021) 110908.
27. A. Salmasifar, M. Edraki, E. Alibakhshi, B. Ramezanzadeh, G. Bahlakeh, Journal of Molecular Liquids **327** (2021) 114856.
28. A. Mustafa, Z.S. Abdullahe, F.F. Sayyid, M.M. Hanoon, A.A. Al-Amiery, W.N.R.W. Isahak, Prog. Color. Color. Coat. **15** (2023) 285.
29. I.A. Kartsonakis, C.A. Charitidis, Appl. Sci. **10**(18) (2020) 6594.
30. D. Neff, L. Bellot-Gurlet, P. Dillmann, S. Reguer, L. Legrand, J. Raman Spectrosc. **37**(10) (2006) 1228.
31. J. Xia, D. Wang, P. Liang, D. Zhang, X. Du, D. Ni, Z. Yu, Biophys. Chem. **256** (2020) 106282.
32. B.D.A. Mistry, Handbook of Spectroscopic Data Chemistry, Oxford Book Company, Jaipur, (2009).